Robotica (2009) volume 27, pp. 701–713. © 2008 Cambridge University Press
doi:10.1017/S0263574708005079 Printed in the United Kingdom

The simplest passive dynamic walking model with toed feet: a parametric study

R. Prasanth Kumar†, Jungwon Yoon†*, Christiand† and Gabsoon Kim‡

†*Intelligent Robots and Systems Lab, School of Mechanical and Aerospace Engineering and ReCAPT, Gyeongsang National University, Jinju, South Korea.*
‡*Department of Control Instrumentation Engineering, Gyeongsang National University, Jinju, South Korea.*

(Received in Final Form: August 11, 2008. First published online: September 11, 2008)

SUMMARY
This paper presents a passive dynamic walking model with toed feet that can walk down a gentle slope under the action of gravity alone. The model is the simplest of its kind with a point mass at the hip and two rigid legs each hinged at the hip on the one end and equipped with toed foot on the other end. We investigate two cases of the model, one with massless legs and another with infinitesimal leg masses. Rotation of the stance foot about the toe joint is initiated by ankle-strike, which is caused by the inelastic collision of the stance leg with a stop mounted on the stance foot. Numerical simulations of walking show that larger step lengths, higher speeds, stability, and energy efficiency can be achieved than what is achievable by a point-feet walker of same hip mass and leg lengths. Period-two gait of a point-feet walker is compared with period-one gait of the toed-feet walker and the mechanism responsible for achieving longer step lengths is described. It is shown that the advantage of the proposed walker comes from its relation to arc-feet walker. The characteristics of deterministic gait with infinitesimal leg masses is compared with that of nondeterministic gait with zero leg masses. It is shown that deterministic gait does not give maximum speed and efficiency compared to nondeterministic gait with swing leg control. Finally, active dynamic walking of the proposed walker is discussed.

KEYWORD: Passive dynamic walking; Biped; Toed feet.

1. Introduction

Human-like gait and energy consumption are two of the main factors to be considered while designing efficient biped robots. Toward this end, current research trend is focused on passive dynamic walking approach as a highly energy efficient model for biped locomotion exhibiting human-like gait. McGeer[1] showed that a passive dynamic walker can walk under the action of gravity on a gentle slope with no actuation and has certain attractive features such as inherent stability of its natural looking gait and very low energy consumption. Following his work, a number of theoretical and experimental studies have been conducted on passive dynamic walking and its application to active dynamic walking on level ground.[2–10]

Most of the passive dynamic walkers studied till date have either arc-shaped feet or point feet. Though arc-feet walkers are better than flat-feet walkers in terms of speed and energy efficiency,[8] arc feet do not look like human feet and are generally statically unstable. Apart from looking natural, flat feet can provide better friction torque and more robustness to floor irregularities. Wisse *et al.*[6] proposed flat feet mounted on ankles with torsional spring stiffness and showed that spring stiffness has similar effect as the foot radius in increasing the robustness to disturbances.

Though flat feet can overcome some of the limitations of arc feet, there is still scope for further improvement not only in more human-like appearance but also in step length, speed, and energy efficiency. A growing number of papers in humanoid robotics indicate the usefulness of toe joint for natural human-like gait in the case of humanoid robots.[11,12] Experiments on humanoid robots with active toe joints showed advantages like ability for knee down motion, higher step climbing, higher speeds etc.[13] Sellaouti *et al.*[14] showed that faster and smoother walking can be achieved using passive toe joints also. The ability to take longer step lengths comes from the extension of the unloading leg possible by rotation of trailing foot about the toe joint.[15] Though the role of toe joints in humanoid robots have been studied experimentally and their benefits have been identified, a similar study from passive dynamic walking point of view is lacking. Such a study is important not only to better understand the complex process of human locomotion but also to build efficient and more human-like biped/humanoid robots.

In this paper, we propose and study a passive dynamic walker model with flat feet that has toe joints. Our chief motivations are human-like foot with no rolling contact with the ground and natural looking gait. To keep the model as simple as possible, we use ankle-strike as a mean to progress to toe-rotation phase. Ankle-strike is defined as an impact of the stance leg against an inelastic stop mounted on the foot such that rotation of the stance leg about the ankle joint is abruptly stopped after a prescribed stance leg angle. It

* Corresponding author. E-mail: jwyoon@gnu.ac.kr

https://doi.org/10.1017/S0263574708005079 Published online by Cambridge University Press

is interesting to note that, in spite of two impact losses per step, the overall energy consumption is quite lower than that of point-feet walkers. By having feet with toe joints, the efficiency of arc-shaped feet is preserved to a large extent. We show through numerical simulations that the proposed walker is more efficient compared to a point-feet walker in terms of speed, energy, and longer step lengths. A discussion on period-two gait in point-feet walkers is presented and its application in our toed-feet walker is explained. We hypothesize that the advantages of the proposed walker come from its relation to arc-feet walker. We also describe a toed-foot walker model with deterministic gait and show that higher speed and energy efficiency are possible with active swing leg control. An analysis of global and local stability is presented for deterministic gait. Finally, study of zero moment point (ZMP) for active dynamic walking is also presented.

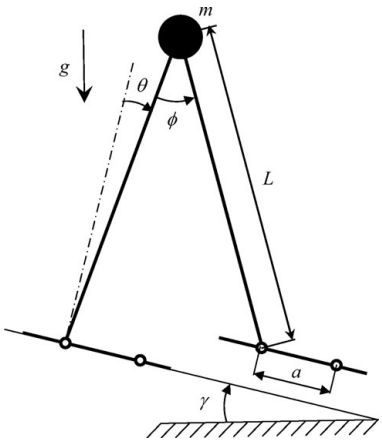


Fig. 1. Passive dynamic walker model with flat feet and toe joints.

2. The Walking Model

A point hip mass with two rigid, straight, and massless legs with infinitesimal point masses at the feet is regarded as the simplest walking model.[4,5,16] In reality, this situation occurs when the hip mass is very large compared to the leg masses, so that the effect of swing leg dynamics on stance leg becomes negligible. Infinitesimal point masses at the feet make the model deterministic, leaving only the slope as the free parameter that uniquely determines the gait. While the swing leg motion depends on the stance leg motion and the slope, stance leg motion is uniquely determined by slope only. Wisse *et al.*[17] showed that the basin of attraction (stability margin) of the simplest walker is very small, but can be significantly extended through swing leg control regardless of the way it is implemented, and devised a simple rule for swing leg control to prevent the walker from falling: *"You will never fall forward if you put your swing leg fast enough in front of your stance leg. In order to prevent falling backward the next step, the swing leg shouldn't be too far in front."* Hence, we first focus our study on stance leg motion assuming that the swing leg is brought in front of the stance leg such that heel-strike occurs at the desired step length and at a time instant which is neither too long nor too short. Given a step length, how to determine the time instant if stable gait exists is discussed under Section 2.5.

We extend the simplest model with point feet by including toed feet to investigate the behavior under toe joint rotation. Figure 1 shows the schematic illustration of the model with notation, where L is the length of the leg, a is the distance between the ankle joint and the toe joint, and m is the mass of the biped. Since none of the joints are actuated, the stance foot does not rotate about the toe joint on its own under the action of gravity. Though it is possible to initiate toe rotation using ankle spring of sufficient stiffness, we choose to use ankle-strike for simplicity. This can be achieved by introducing an inelastic stop and a locking mechanism between the leg and the foot, so that after a prescribed stance leg angle θ_{A-}, the stance leg and the stance foot are locked together after impact and rotate about the toe joint with common angular velocity. As a consequence of using toed feet with massless legs, there are three free parameters for the proposed walker that uniquely define the gait, namely, slope, step length, and stance leg angle at which ankle-strike occurs. This collision as well as the heel-strike are assumed to be perfectly inelastic with angular momentum conserved. Thus, for every step there are two impact losses. Brief foot scuffing of swing leg at midstance is ignored as is generally done for compass gait bipeds.[2] The various phases and transitions involved in walking are shown in Fig. 2. The portions of the foot behind the ankle joint and toe joint are necessary for active walking due to ZMP constraint, but not required for passive walking. The equations of motion and transition are detailed as follows.

2.1. Ankle-rotation phase

During ankle-rotation phase, the stance leg rotates about the ankle joint. The stance leg is modeled as a simple inverted pendulum with ankle joint as pivot. The equation of motion

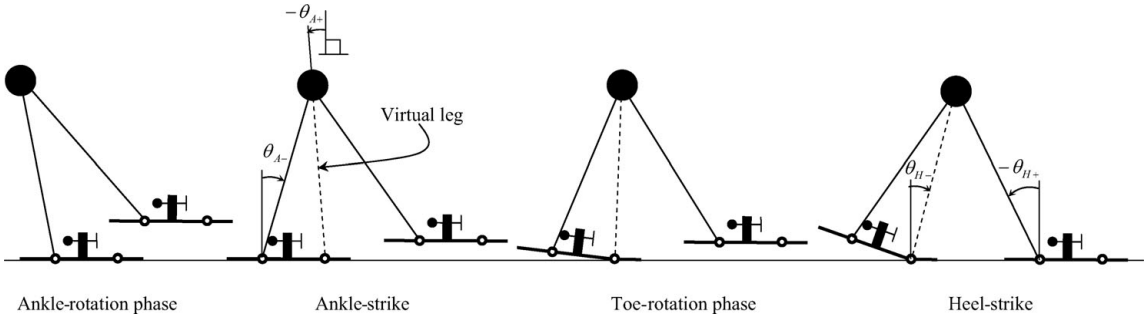


Fig. 2. Phases and transitions during walking shown with adjustable hard stops on the feet.

https://doi.org/10.1017/S0263574708005079 Published online by Cambridge University Press

of the stance leg is given by

$$\ddot{\theta} = \frac{g}{L}\sin(\theta + \gamma), \tag{1}$$

where θ is the angle made by the stance leg with the vertical to the incline, and γ is the slope of the incline. This equation is valid from heel-strike to ankle-strike.

2.2. *Ankle-strike*

The ankle-rotation phase ends with the ankle-strike caused by the inelastic collision of the stance leg with a stop mounted on the stance foot. Ankle-strike can be made to occur at any desired stance leg angle by means of an adjustable stop. The ankle is locked immediately after collision. This ensures that the collision is inelastic. Ankle-strike results in rotation of the stance foot (along with the stance leg) about the toe joint. This is equivalent to the effect produced by a rigid massless leg (virtual leg) joining the hip joint and the toe joint colliding the ground at the toe joint. Hence, the angular momentum of the walker is conserved about the toe joint. Let θ_{A-} be the stance leg angle at which ankle-strike occurs. Before ankle-strike, let L_{A-} be the length of the effective leg defined as the line joining the hip joint to the pivot point which is the ankle joint. Hence, this is same as the actual leg length L. After ankle-strike, the toe joint becomes the pivot about which the walker rotates. The effective leg in this case becomes the line joining the hip joint and the toe joint. We call this as virtual leg, the length of which can be determined through cosine rule as

$$L_{A+} = \sqrt{L_{A-}^2 + a^2 - 2L_{A-}a\sin\theta_{A-}}. \tag{2}$$

We define θ_{A+} as the angle made by the virtual leg with the vertical of the inclined plane just after ankle-strike. Using simple geometry and sign convention (clockwise positive from vertical), this can be derived as

$$\theta_{A+} = \mathrm{sgn}(L_{A-}\sin\theta_{A-} - a)\arccos\left(\frac{L_{A-}}{L_{A+}}\cos\theta_{A-}\right). \tag{3}$$

In general, $\theta_{A+} \neq -\theta_{A-}$ unless

$$L_{A+} = L_{A-}.$$

Conservation of angular momentum about the toe joint gives the transition equation as

$$\dot{\theta}_{A+} = \frac{L_{A-}}{L_{A+}}\dot{\theta}_{A-}\cos(\theta_{A-} - \theta_{A+}), \tag{4}$$

where $\dot{\theta}_{A-}$ is the angular velocity of the stance leg just before ankle-strike and $\dot{\theta}_{A+}$ is the angular velocity of the virtual stance leg just after ankle-strike.

2.3. *Toe-rotation phase*

After ankle-strike, the walker is supported by the virtual leg and the entire walker rotates about the toe joint. The equation of motion in this case becomes

$$\ddot{\theta} = \frac{g}{L_{A+}}\sin(\theta + \gamma). \tag{5}$$

This equation is valid till heel-strike.

2.4. *Heel-strike*

Heel-strike occurs when the swing foot touches the ground (i.e., inclined plane). The swing leg is assumed to be controlled [17] to maintain the time instant of heel-strike for the desired step length such that the gait is stable. We also assume that the swing foot is parallel to the ground at heel-strike with zero horizontal relative velocity. Conservation of angular momentum at heel-strike gives the transition equation as

$$\dot{\theta}_{H+} = \frac{L_{A+}}{L}\dot{\theta}_{H-}\cos(\theta_{H-} - \theta_{H+}), \tag{6}$$

where θ_{H-} and $\dot{\theta}_{H-}$ are the virtual stance leg angle and its angular velocity just before heel-strike, and θ_{H+} and $\dot{\theta}_{H+}$ are the stance leg angle and its angular velocity just after heel-strike.

2.5. *Limit cycles*

A limit cycle in passive dynamic walkers refers to the periodicity of gait which occurs when the initial conditions of any step is exactly same as the initial conditions of the next step. For the proposed walker, the initial conditions are the stance leg angle and the stance leg angular velocity just after heel-strike, i.e., at the beginning of a new step. Limit cycles of the proposed walker model can be determined as follows. Let L_s be the step length. Let E_{A-}, E_{A+}, E_{H-}, and E_{H+} are the pre- and postimpact energy levels at ankle- and heel-strikes. Then, the following condition holds for cyclic gait:

$$\begin{aligned}&\text{Potential energy loss for one step}\\ &= \text{Energy loss at ankle-strike}\\ &\quad + \text{Energy loss at heel-strike},\end{aligned} \tag{7}$$

$$mgL_s\sin\gamma = (E_{A-} - E_{A+}) + (E_{H-} - E_{H+}). \tag{8}$$

Since, only kinetic energy is lost during collisions,

$$\begin{aligned}mgL_s\sin\gamma &= \frac{1}{2}mL^2\dot{\theta}_{A-}^2 - \frac{1}{2}mL_{A+}^2\dot{\theta}_{A+}^2\\ &\quad + \frac{1}{2}mL_{A+}^2\dot{\theta}_{H-}^2 - \frac{1}{2}mL^2\dot{\theta}_{H+}^2 \qquad (9)\\ &= \frac{1}{2}mL^2\left(\dot{\theta}_{A-}^2 - \dot{\theta}_{H+}^2\right)\\ &\quad + \frac{1}{2}mL_{A+}^2\left(\dot{\theta}_{H-}^2 - \dot{\theta}_{A+}^2\right). \qquad (10)\end{aligned}$$

Similarly, potential energy loss during ankle-rotation phase is equal to kinetic energy gain from post-heel-strike to

https://doi.org/10.1017/S0263574708005079 Published online by Cambridge University Press

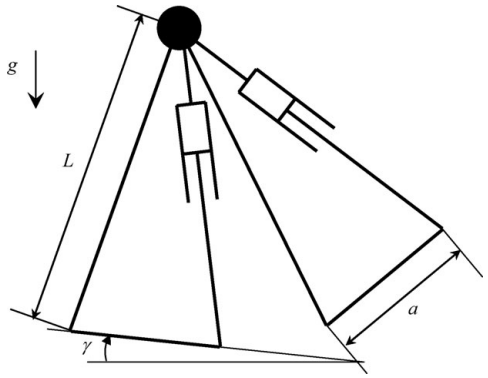


Fig. 3. Equivalent model of the passive dynamic walker.

pre-ankle-strike.

$$mgL(\cos(\theta_{H+}+\gamma)-\cos(\theta_{A-}+\gamma))=\frac{1}{2}mL^2\left(\dot{\theta}_{A-}^2-\dot{\theta}_{H+}^2\right). \quad (11)$$

Given the step length L_s, the only independent variable that determines a unique gait for this slope is the angle at ankle-strike θ_{A-}. Other angles θ_{A+}, θ_{H-}, and θ_{H+} can be determined from L_s and θ_{A-} through simple geometric relations (see Fig. 2). From (4), (6), (10), and (11) one can determine $\dot{\theta}_{H+}$. The validity of this solution, i.e., whether the obtained initial conditions θ_{H+} and $\dot{\theta}_{H+}$ satisfy periodicity condition, can be verified by integrating (1) and (5) using the transition equations (4) and (6). If the periodicity condition is not satisfied, it means the combination of the free gait parameters L_s, θ_{A-}, and γ do not give stable gait.

Since the swing leg trajectory between heel-strike impacts does not influence the stance leg trajectory, it can be arbitrarily designed but satisfying the end conditions of the step length.

2.6. *Equivalent model*

The equivalent model of the proposed biped is as shown in Fig. 3. The physical leg length is denoted by L, and the virtual leg length is denoted by L_v which is determined based on the desired ankle angle. Two steps of this equivalent model is equal to one step of original biped model. Though this is a two-legged robot, it behaves as a four-legged one with a constant distance of a between the tips of actual leg and its corresponding virtual leg.

3. Results

The model parameters for walking simulation are given in Table I. Limit cycles leading to stable gaits are determined through the procedure mentioned in the previous section. Given the mass m, leg length L, and the distance between ankle and toe joints a, we have three free parameters

Table I. Model parameters.

m	10 Kg
L	0.5 m
g	9.81 m/s^2

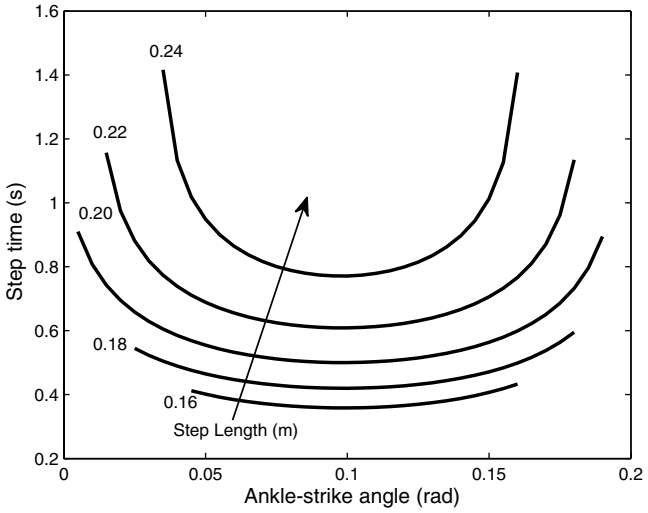


Fig. 4. Step time vs. ankle-strike angle for increasing step lengths on a slope of $\gamma = 0.004$ rad and $a = 0.1$ m.

that uniquely determine the gait: slope, step length, and ankle-strike angle. Additionally, we will also consider the parameter a in our study to determine its overall influence on gait.

3.1. *Step period*

Step period shows considerable variation with respect to ankle-strike angle as shown in Fig. 4 for a slope of $\gamma = 0.004$ rad and $a = 0.1$ m. The variation is higher at higher step lengths. The step period is found to increase with the increase in step length. This is quite natural to expect; longer steps need more time.

For each step length, it can be noted that the step period is lowest near an ankle-strike angle of 0.1 rad. This angle corresponds to the case of virtual leg length equal to the physical leg length.

Stable gaits do not exist for extreme values of ankle-strike angle. The range of ankle-strike angles for which stable gaits can be found is maximum for a step length of 0.2 m. This is double the distance between ankle and toe joints.

3.2. *General rimless wheel*

Rimless wheel is a spoked wheel with the rim removed.[1,18] We have already noted that ankle-strike angle which gives a virtual leg length equal to the physical leg length has the advantage of very low step periods. With uniform leg lengths, it is possible to view the walker as a part of a spoked wheel. Thus, a general rimless wheel can be defined as the one whose spokes represent the virtual and the physical legs of the walker alternately as shown in Fig. 5. The inter-leg angle need not be uniform for such a rimless wheel.

In fact, when the inter-leg angle is uniform it reduces to the well-known rimless wheel as shown in Fig. 6. However, the interpretation of the rolling motion is slightly different. Two steps taken by the rimless wheel correspond to one step taken by the proposed walker, the first step being taken by the virtual leg with step length equal to a, and the second by the new stance leg with step length equal to $L_s - a$, where

https://doi.org/10.1017/S0263574708005079 Published online by Cambridge University Press

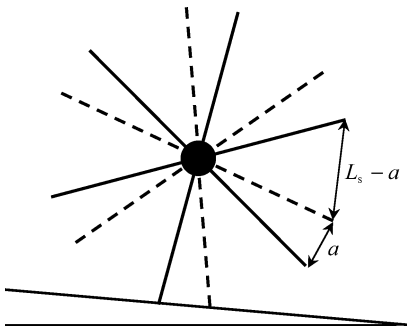


Fig. 5. Rimless wheel with unequal inter-leg angles; virtual legs are represented by dashed lines. The total step length $L_s = a + (L_s - a)$.

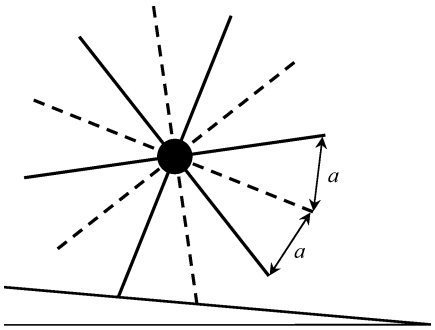


Fig. 6. Rimless wheel with uniform inter-leg angle; virtual legs are represented by dashed lines. The total step length $L_s = 2a$.

L_s is the step length for one step of the proposed walker. For equal inter-leg angles, $L_s - a = a$, or $L_s = 2a$.

With fixed values of a, results plotted in Fig. 7 for a slope of $\gamma = 0.004$ rad show that the maximum speed occurs at a step length which is nearly 1.5 times the distance between ankle and toe joints. This value is slightly lower for lower values of a. This indicates that for attaining maximum speed there exists a preferred step length for a given value of a.

With fixed values of L_s, results plotted in Fig. 8 show that for all the step lengths the maximum speed occurs when a is half of the step length. These results, for fixed a and fixed L_s, are not contradictory. This can be better understood from Fig. 9. For $a = 0.1$ m, preferred L_s is 0.146 m. For a step length L_s of 0.146 m, the preferred value of a is 0.073 m but not 0.1 m which gives lesser speed. Similarly, for a step length L_s of 0.2 m, the preferred value of a is 0.1 m. The

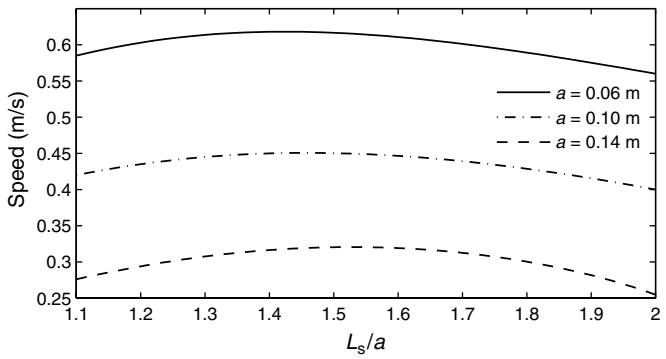


Fig. 7. Speed vs. L_s/a for a slope of $\gamma = 0.004$ rad for fixed a.

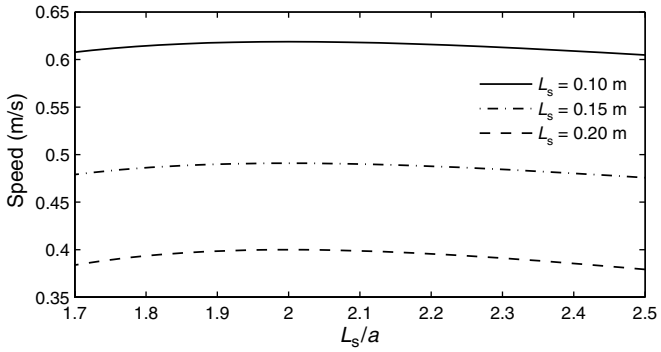


Fig. 8. Speed vs. L_s/a for a slope of $\gamma = 0.004$ rad for fixed L_s.

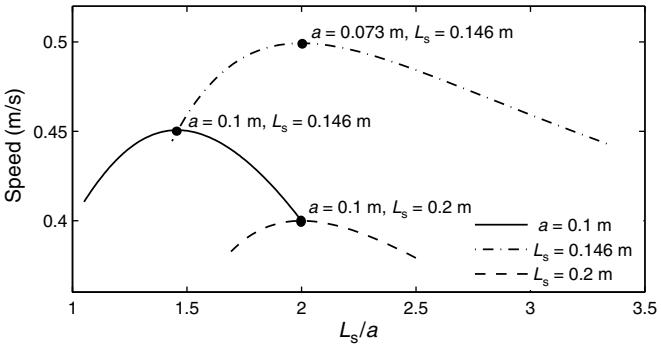


Fig. 9. Speed vs. L_s/a for a slope of $\gamma = 0.004$ rad.

values of a or L_s which give maximum speed depends on which one of them is fixed and which one is free to change.

Hence, if we are to design a toed-feet walker for a nominal step length, in order to obtain maximum speed for that step length the distance between ankle and toe joints needs to be chosen as half of the step length. However, when there is no constraint on step length, the best step length that can be chosen for the designed value of a can be determined from Fig. 7.

3.3. Intermediate steps

It is well known that for any given slope the walking speed increases with decreasing step length or inter-leg angle.[1] This fact finds an application in the proposed walker. For example, consider a slope of $\gamma = 0.01$ rad, and a step length L_s of 0.2 m. For the case of point-feet walker, stable periodic gait is obtained for initial conditions $\theta = -0.2014$ rad and $\dot{\theta} = 0.93$ rad/s, with a corresponding step time of 0.712 s. In order to obtain the same step length, the proposed toed-feet walker takes intermediate step with the virtual leg, thus effectively decreasing the inter-leg angle. In this case stable periodic gait is obtained for initial conditions $\theta_{H+} = -0.1002$ rad and $\dot{\theta}_{H+} = 1.3796$ rad/s, with a corresponding step time for traversing the step length L_s as 0.2978 s. As a result of smaller inter-leg angles the time taken is less than half of what is required by a point-feet walker.

3.4. Energy efficiency

One can clearly see that using toe joints is more efficient in view of speed. However, the cost of transport (COT) or specific resistance,[1,19] defined as the energy required to carry

https://doi.org/10.1017/S0263574708005079 Published online by Cambridge University Press

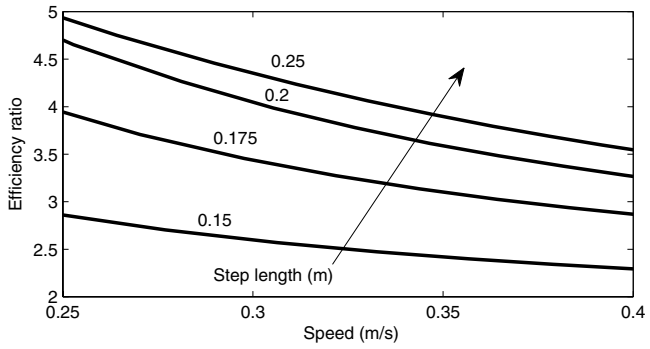


Fig. 10. Efficiency ratio of proposed walker with respect to point-foot walker calculated at identical speeds and step lengths.

a unit weight for unit distance, is same in both the cases when compared for the same slope because the value of COT is given by slope itself. As the biped moves down the slope, all the potential energy is lost in impacts. For traversing every step length, the potential energy converted to kinetic energy and loss in impacts is equal for both the cases. However, the toed-feet walker consumes more power and moves faster. Hence, it is more appropriate to compare energy efficiencies for the same speed. In the previous example, we reduce the slope to $\gamma = 0.002345$ rad in order to reduce the speed so that the step length and step time are same as that of the point-feet walker. Stable periodic gait is obtained for initial conditions of $\theta_{H+} = -0.1002$ rad and $\dot{\theta}_{H+} = 0.6681$ rad/s. Thus, for this example, the proposed walker is nearly four times more energy efficient than a point-feet walker.

Figure 10 shows the efficiency ratio of the proposed walker with respect to a point-foot walker calculated at identical speeds and step lengths. Efficiency ratio is defined as the ratio of cost of transports of the point-feet walker $\tan\gamma_p$ and that of the proposed toed-feet walker $\tan\gamma_t$ calculated at the same speed and step length. As shown in Fig. 10, the proposed walker is more efficient than a point-feet walker at all speeds. The efficiency is higher at lower speeds indicating the higher ability of the proposed walker to take longer steps even at lower speed. With the decrease in step length, the effectiveness drops off sharply. For step length equal to a, the performance is no better than a point-feet walker. In fact, it is not possible to use the toe joint for $L_s \leq a$. The effectiveness of the walker depends on its ability to take intermediate steps using its virtual legs which is not possible for $L_s \leq a$.

3.5. Application of period-two gait of point-feet walker

Period-one gait is defined as a gait in which the walker returns to the same initial conditions for each step. Similarly, period-two gait is defined as a gait in which the walker returns to the same initial conditions after two consecutive steps. Period-two gait of a point-feet walker is equivalent to the period-one gait of the proposed walker with virtual leg length equal to the actual leg length and appropriate values for the parameters a, and L_s. This directly follows from the fact that each step of the proposed walker has to be interpreted as two steps of a point-feet walker, one taken by the virtual leg and another by the new stance leg.

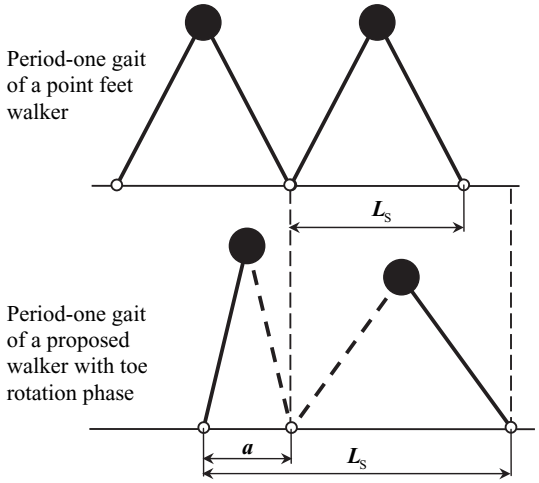


Fig. 11. Period-one gaits of a point-feet walker and the proposed walker for their respective maximum step lengths on a slope of $\gamma = 0.004$ rad. $L_s = 0.157$ m for the point-feet walker, and $L_s = 0.275$ m for the proposed walker. The second phase of the proposed walker's step is exaggerated for comparison.

The advantage of period-two gait can be found in the ability of the walker to take longer steps. For example, the maximum step length for stable period-one gait for a point-feet walker on a slope of $\gamma = 0.004$ rad is 0.157 m. The maximum step length possible for the proposed walker is 0.275 m with $a = 0.1$ m. About 75% longer steps are possible for this example.

It can be observed that each of the transitions between the two phases (i.e, ankle joint rotation and toe joint rotation) can be thought of as belonging to some gait of a point-feet walker with their respective step lengths, a and $L_s - a$. Both of these point-feet gaits are individually unstable. For example, consider the previous case of maximum possible step lengths. Point-feet walker has 0.157 m whereas the proposed walker has 0.275 m. The maximum step length of the proposed walker can be split into 0.1 m corresponding to a, and 0.175 m corresponding to $L_s - a$ as shown in Fig. 11. Clearly, the step length of the second transition phase is more than what is possible (stably) by the point-feet walker. Yet, it is a part of a stable gait of the proposed walker.

This can be explained by considering the energy transfer between the two gait phases in each step. The first phase has more energy than required to maintain a steady gait with step length of a. If it continues, it will fall back to correct energy level by dissipating excess energy. The second phase individually does not have enough energy to maintain a steady gait with step length $L_s - a$. Therefore, it is bound to stop. When the excess amount of energy is transferred from the first phase to the second phase, they can alternate indefinitely producing a period-two gait. This is also referred to as bifurcation[2] or limping.[4] Though it is a period-two stable gait for a point-feet walker, it has to be treated as a period-one stable gait for the proposed walker.

4. Relation to Arc-Shaped Feet

In this section, we will show how the proposed toed-foot is related to the arc-shaped foot with respect to physical shape as well as efficiency.

https://doi.org/10.1017/S0263574708005079 Published online by Cambridge University Press

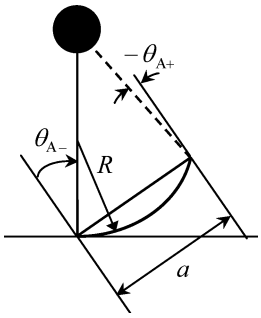


Fig. 12. Toed foot as a discretization of arc foot.

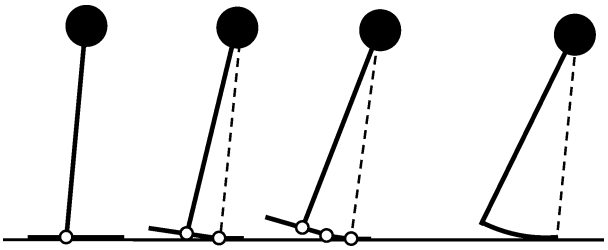


Fig. 14. Arc-foot as a limiting case of the proposed foot.

4.1. Efficiency lies between arc-feet walker and point-feet walker

It is well known that passive dynamic walkers with arc-shaped feet are more efficient compared to point-feet walkers.[1] Synthetic wheel, which has arc-radius equal to the leg length, has zero COT since ideally there are no impact losses. Point foot is a special case of arc foot with zero radius. Therefore, there always exist arc-feet walkers of some radii whose costs of transports are less than that of the toed-feet walker. Hence, the efficiency of the proposed model lies in between that of arc-feet walker of some radius and point-feet walker.

4.2. Proposed foot is a discretization of arc foot

A toed foot can be seen as a coarse discretization of an arc foot of some radius which depends on ankle-strike angle and the distance between ankle and toe joints as shown in Fig. 12. Generally, discretization of a continuous entity results in an approximation of the continuous entity in some or all of its properties. In the present case, we claim that discretization of arc foot as toed foot results in approximation of walking efficiency. This can be explained from Fig. 13 which shows the center of mass trajectories for the proposed walker with $a = 0.1$ m and a point-feet walker both walking with the same step length. From the figure it is clear that for the same step length, the angle between pre-impact and postimpact center of mass velocities is less for ankle- and heel-strikes in the case of the proposed model compared to that of heel-strike in the case of point-feet walker. In general, the lower this angle, the lesser is the impact loss.[20] Apart from this angle, the actual losses depend on the magnitude of velocities before these impacts. The combined energy loss due to ankle and heel impacts in toed-feet walker is equal to the energy loss due to heel-strike alone in point-feet walker because they lose same amount of potential energy per step at the same slope and step length.

In the previous sections it has been shown that the proposed walker walks faster than the point-feet walker at the same slope and step length. For a fair comparison, the slope on which the proposed walker walks has to be reduced to match the speed of the point-feet walker keeping the step length same. Then, the COT and hence the energy consumed per step will be lower than that of the point-feet walker. Therefore, it can be concluded that the combined energy loss for ankle- and heel-strikes in the toed-feet walker is lower than the energy loss due to heel-strike in the point-feet walker when both these walkers move at the same speed with same step length. This conclusion has already been reached through numerical simulations in Fig. 10. The point we want to make here is, in spite of two impacts per step length the overall energy loss in impacts is lower due the reasons described earlier, and this increase in energy efficiency occurs as a result of discretization of arc foot.

This idea can be more clearly understood by considering discretization to finer levels leading to a foot with a chain of joints that can better approximate an arc foot of any given radius by appropriately setting the desired angles at which the impacts take place. With more number of joints the total loss of energy in impacts for all the joints will be lesser than the energy loss with one joint. This follows from the same reasoning given earlier. The angles between pre-impact and postimpact center of mass velocity vectors for each impact occurring within the foot are reduced. In the limit, such infinite joints as shown in Fig. 14 reduce the impact losses occurring within the foot to zero making the foot identical to arc foot. However, loss of energy due to heel-strike, which occurs outside the foot, remains the same.

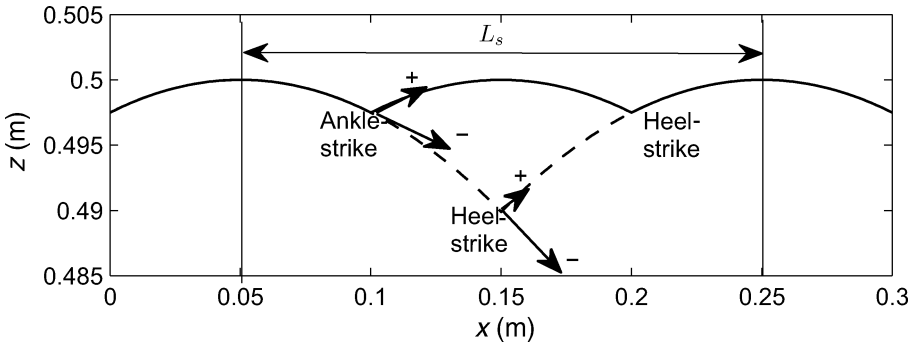


Fig. 13. Comparison of the path of center of mass for a step length of 0.2 m. Dashed line, point-feet walker; solid line, proposed walker.

https://doi.org/10.1017/S0263574708005079 Published online by Cambridge University Press

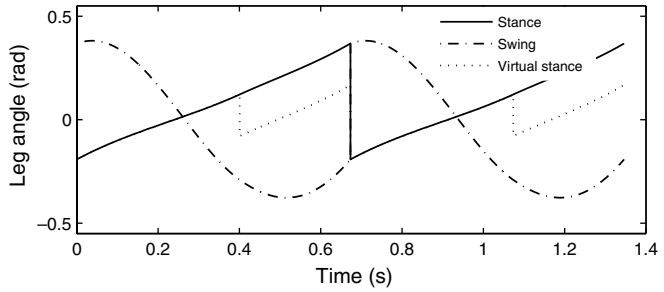


Fig. 15. Leg angle trajectories for two steps.

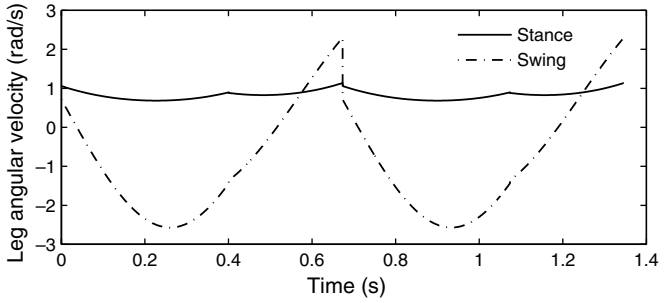


Fig. 16. Leg angular velocity trajectories for two steps

5. Simplest Model with Deterministic Gait

Adding infinitesimal masses to the legs makes the gait deterministic, with both the stance and swing leg trajectories uniquely determined by the system parameters.[4] The advantage comes from the fact that, unlike in nondeterministic gait, the system becomes autonomous with no necessity to design swing leg trajectory and a trajectory tracking controller to track the swing leg trajectory.

The equations of motion and the associated transition equations for deterministic gait are given in the appendix. Typical leg angle and angular velocity trajectories for a slope of 0.5° with an ankle-strike angle of 7° are shown in Figs. 15 and 16. The instant of ankle-strike cannot be clearly seen in Fig. 15 because the angle trajectory is continuous. The angular velocity trajectory, however, is discontinuous at ankle- and heel-strike impacts, as can be seen in Fig. 16. The discontinuity at ankle-strike is very small compared to the discontinuity at heel-strike, indicating a small kinetic energy loss. The phase plot of the limit cycle is shown in Fig. 17.

It is interesting to note that for a given ankle-strike angle, nature "chooses" a particular passive gait with step length and step period that do not give the highest possible walking speed as can be seen in Fig. 18. The range of feasible ankle-strike angles is also low for the deterministic gait. The situation can be dramatically improved by swing leg control as shown in Fig. 18. However, the effort required to control the swing leg can increase if the controlled swing leg trajectory does not match with the passive swing leg trajectory, especially when the leg mass is appreciable.

6. Stability

6.1. Global stability

The basin of attraction of a biped walker is a measure of its global stability. It is the set of all initial states which lead

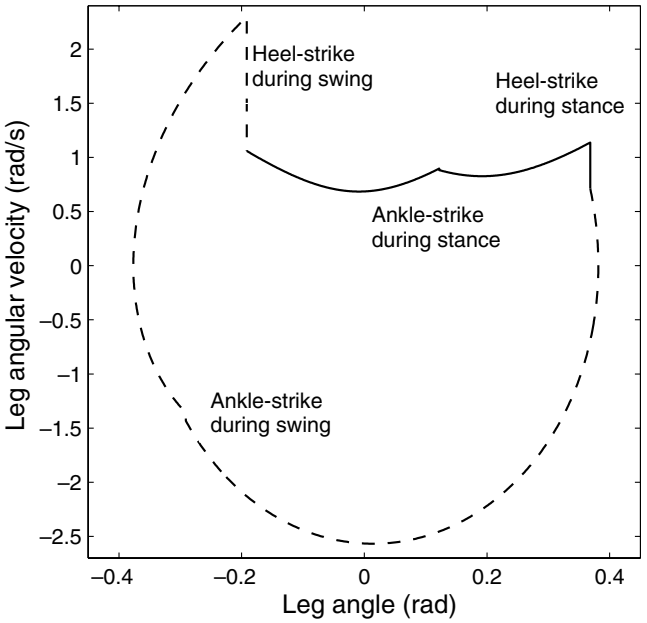


Fig. 17. Phase plot of the limit cycle; stance phase ——, swing phase – –.

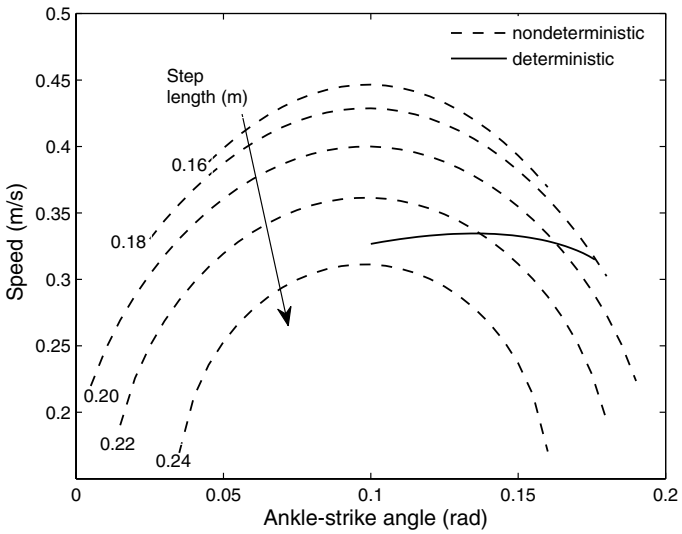


Fig. 18. Speed vs. ankle-strike angle for various step lengths of deterministic and nondeterministic gaits at a slope of 0.004 rad.

to the convergence of the gait to a stable limit cycle. It can be significantly increased with swing leg control.[17] Much smaller basin of attraction is obtained with passive swing leg motion. However, by adding a toed foot, the basin of attraction can be considerably increased. Figure 19 shows a section basin of attraction in the plane of fixed point, where the limit cycle converges. The fixed point is shown by an asterisk in the figure. The plot shows swing leg angular velocity versus swing leg angle with dark cells representing stable initial conditions which lead to the fixed point. Comparing this with Fig. 20, we can say that the proposed walker is more stable than a point-foot walker. The size of basin of attraction does not vary much with the variation of ankle-strike angle. However, there is noticeable increase with respect to increase in the distance between ankle and toe joints as shown in Fig. 21.

https://doi.org/10.1017/S0263574708005079 Published online by Cambridge University Press

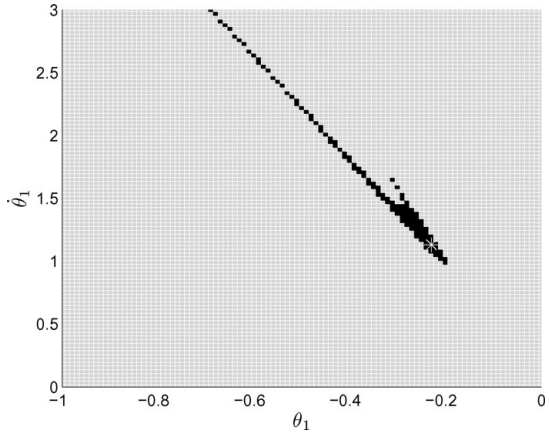


Fig. 19. Fixed plane section of basin of attraction for point-foot walker on a slope of 1°.

6.2. Local stability

Given that the initial conditions of the walker fall within the basin of attraction, local stability is determined by the rate of convergence or how fast the walker approaches its limit cycle. Maximum singular value of the linearized Poincaré map gives an indication of rate of convergence.[7] Rate of convergence is inversely proportional to the maximum singular value.

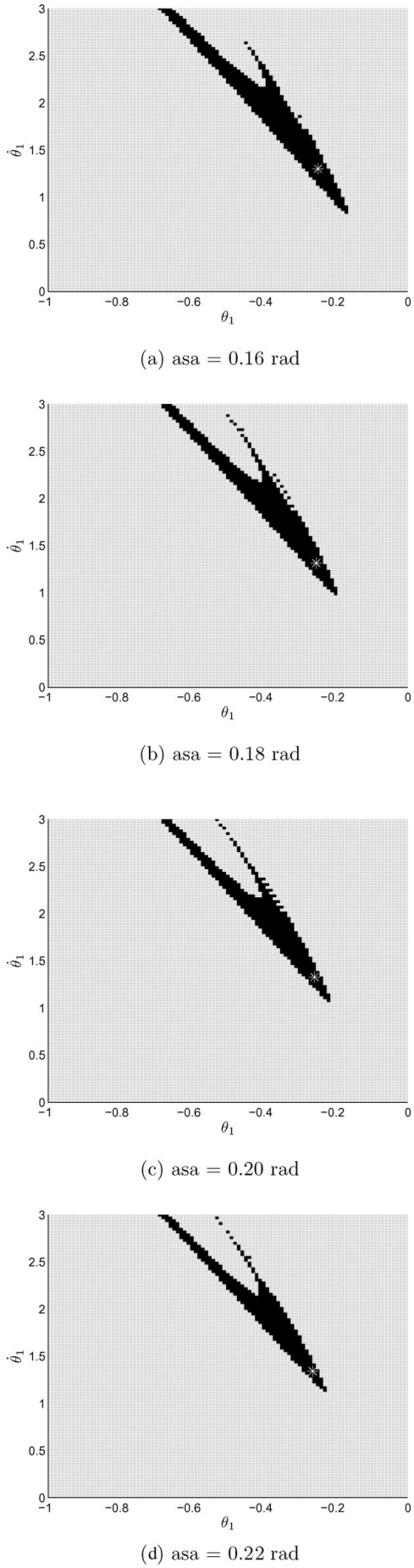
For the proposed biped walker model, the rate of convergence is expected to be higher than that of point-feet walker because of the intermediate steps taken through virtual legs. However, it can vary depending on the ankle-strike angle as shown in Fig. 22. The maximum singular value decreases gradually up to a certain walking speed and then increases rapidly. There exists a speed at which it is minimum indicating maximum stability. Results show that comparatively higher convergence rate can be achieved with the proposed toed-foot walker for certain speeds depending on the the ankle-strike angle. Hence, for a given speed, ankle-strike angle can be appropriately chosen such that not only efficiency but also stability is maximized.

7. Active Dynamic Walking on Level Ground

The ultimate objective of studying passive dynamic walkers is to develop highly efficient active dynamic walkers. The gait of passive dynamic walkers requires very low energy inputs through gravity. Realization of passive dynamic gait for active dynamic walkers on level ground can be easily done using the concept of virtual gravity.[7] Imagine a virtual gravity field defined by an acceleration of $g/\cos\gamma$, under which the biped robot exhibits passive walking with steady gait. Typical gait of the walker is as shown in Fig. 23. Hip joint torque is negligible compared to the ankle or toe joint torque, and hence it does not influence the ZMP.

7.1. Efficiency

Compared to a flat-foot walker (equivalent of point-foot walker for active walking), the COT of the proposed walker in active walking is always lower because of the lower virtual slopes needed to achieve the same speed as that of the flat-foot walker. The analysis and the results of costs of transport,



(a) asa = 0.16 rad

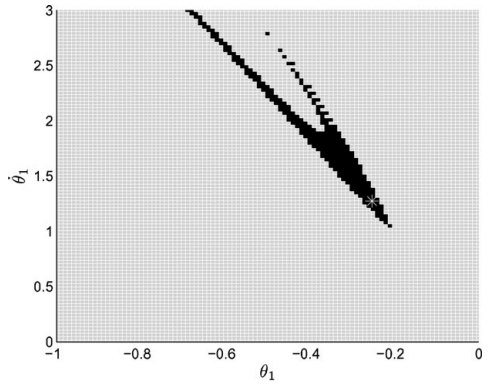
(b) asa = 0.18 rad

(c) asa = 0.20 rad

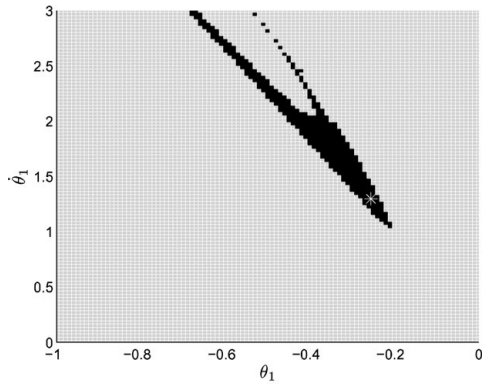
(d) asa = 0.22 rad

Fig. 20. Fixed plane section of basin of attraction for various values of ankle-strike angle (asa) with $c = 0.1$ m on a slope of 1°.

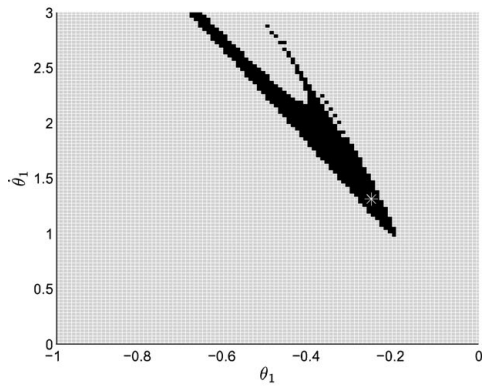
https://doi.org/10.1017/S0263574708005079 Published online by Cambridge University Press



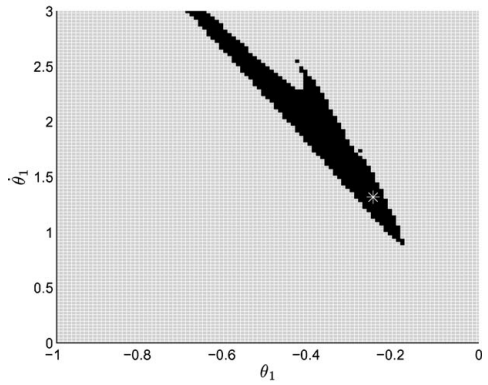
(a) $c = 0.06$ m



(b) $c = 0.08$ m



(c) $c = 0.10$ m



(d) $c = 0.12$ m

Fig. 21. Fixed plane section of basin of attraction for various values of c with asa = 0.18 rad on a slope of 1°.

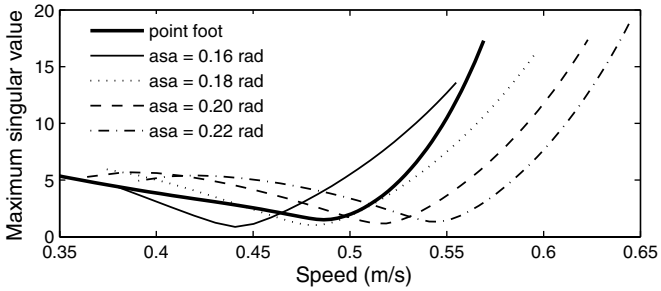


Fig. 22. Maximum singular values vs. speed for point-foot walker and the toed-foot walker for various ankle-strike angles (asa).

speed, and step lengths for the active version of the proposed walker is similar to its passive version.

7.2. The zero moment point

The equation of motion of inverted pendulum model becomes

$$\begin{aligned}\ddot{\theta} &= \frac{g}{L\cos\gamma}\sin(\theta+\gamma)\\ &= \frac{g}{L}\sin\theta + \frac{g}{L}\tan\gamma\cos\theta,\\ \ddot{\theta} &= \frac{g}{L}\sin\theta + \tau, \end{aligned} \tag{12}$$

where $\tau = (g/L)\tan\gamma\cos\theta$ is the joint control input. Actual joint torque is given by $mL^2\tau$, where L is the pendulum length.

Therefore, a virtual gravity field of $g/\cos\gamma$ can be created on level ground using an ankle joint torque of

$$u_{\mathrm{a}} = mgL_{\mathrm{A}-}\tan\gamma\cos\theta \tag{13}$$

during ankle-rotation phase and a toe joint torque of

$$u_{\mathrm{t}} = mgL_{\mathrm{A}+}\tan\gamma\cos\theta \tag{14}$$

during toe-rotation phase.

Using these torques, passive dynamic gait in virtual gravity can be achieved on level ground with the associated passivity property. Though the control torques are not error feedback

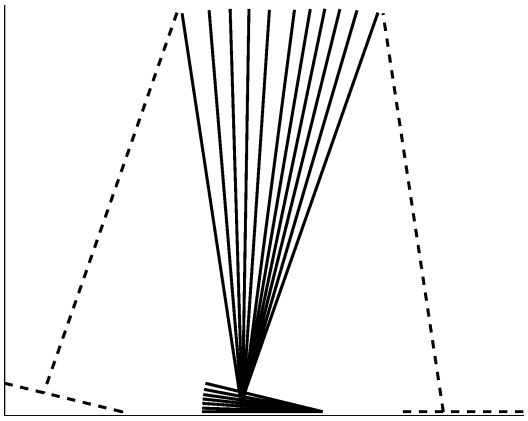


Fig. 23. Stick figure representing a typical gait. Swing leg is shown as dashed line.

https://doi.org/10.1017/S0263574708005079 Published online by Cambridge University Press

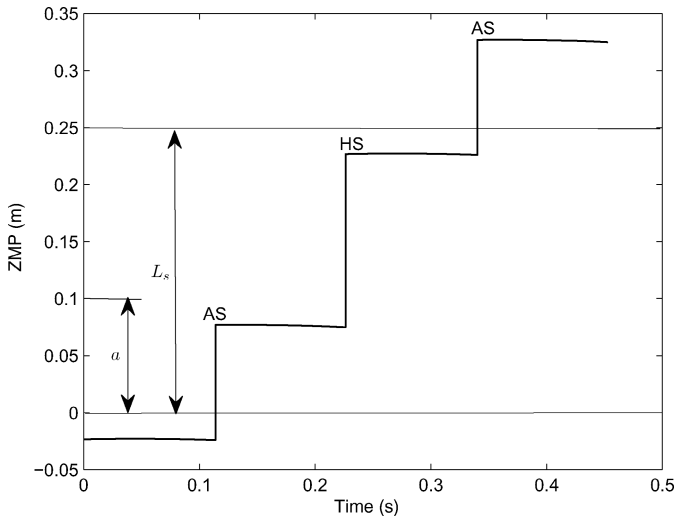


Fig. 24. ZMP trajectory for one step of the proposed model with $a = 0.1$ m and $\gamma = 0.0349$ rad. AS: ankle-strike, HS: heel-strike.

control inputs, the gait can remain stable in the presence of disturbances.

In the case of passive dynamic walking, the ZMP always stays at the pivot point. However, this is no longer true for active walking in a virtual gravity field because of the active torques applied at the pivot points to create virtual gravity. The position of ZMP from the ankle/toe joint in this case is given by

$$x_{\text{zmp}} = -\frac{u}{m(\ddot{z} + g)}, \tag{15}$$

where $\ddot{z}$ is the vertical acceleration of the center of mass and u is the associated joint torque.

From (13) and (14), it can be observed that both ankle and toe joint torques are always positive. The vertical acceleration of the hip mass is significantly lower in magnitude than acceleration due to gravity during normal walking. Hence the denominator is positive in (15). We can see that the position of ZMP is bound to be negative because of the positive denominator term. This shows that the ZMP stays always behind the ankle or toe joint.[7] Therefore, it is necessary to design the toe and the heel to have sufficient area behind their joints to accommodate the range of ZMPs for different gaits. Typical ZMP trajectory for a slope of $\gamma = 0.0349$ rad and $a = 0.1$ m is as shown in Fig. 24. At ankle-strike, the ZMP jumps from the back of the ankle joint to the back of the toe joint, and at heel-strike ZMP jumps from behind the toe joint of stance foot to the back of ankle joint of the new stance foot. It should be noted that the range of ZMP and its distance from the pivot during the ankle-rotation phase and the toe-rotation phase depend on the slope of the virtual gravity field.

8. Conclusions and Future Work

A passive dynamic walker model with flat feet and toe joints has been proposed and a parametric study has been performed. Results show that the proposed model can walk faster than a point-feet walker is capable of taking larger foot steps and is also energy efficient. Fastest walking for a given step length L_s and the distance between ankle and toe joints a occurs when the virtual leg length is close to the actual leg length. For this case, given a step length, maximum speed can be obtained when a is half of the step length. Again, for a fixed a, the maximum speed occurs for a step length of nearly 1.5 times a. The proposed walker is, in general, more energy efficient than a point-feet walker. However, its energy efficiency is more pronounced at lower speeds and higher step lengths.

An application of period-two gaits with symmetric legs of a point-feet walker has been identified in the proposed walker. These period-two gaits occur as period-one gaits in our model. The underlying energy transfer mechanism has been discussed. This explains how the proposed walker is capable of taking longer steps.

The relationship between the proposed foot and an arc-shaped foot has been discussed. It was shown that arc-shaped foot is the limiting case of a foot with a series of toe joints with appropriate impact and lock mechanisms, and the efficiency of the proposed foot lies in between that of the arc-shaped foot of some radius and point foot. The proposed foot is shown to be a discretization of arc foot of some radius determined by ankle-strike angle and the distance between the ankle and toe joints.

A two degrees of freedom model of the toed foot walker with infinitesimal leg masses that is capable of generating deterministic gait has been presented. It was shown that the passive deterministic gait generally does not give the highest speed or efficiency. Swing leg control allows higher speeds, but requires trajectory design and tracking controller. Stability studies indicate that the basin of attraction of the proposed walker is larger and convergence rate to the limit cycle is higher compared to a point-foot walker.

Though our model is quite simple, it captures most of the essential benefits of toe joints. We believe that it will be a good starting point for analyzing more complex models with leg mass, torso etc. A spring may also be included in the ankle lock mechanism so that the ankle is locked after absorbing energy from the leg–ankle relative motion. This energy can be utilized just before heel-strike to reduce impact loss. Release of this energy prior to heel-strike may require additional actuation.[21]

Acknowledgments

This work was supported by the Korea Research Foundation Grant funded by the Korean Government (MOEHRD) (KRF-2005-005-J09902) and was supported by grant no. R01-2006-000-10468-0 from the Basic Research Program of the Korea Science & Engineering Foundation.

References

1. T. McGeer, "Passive dynamic walking," *Int. J. Robot. Res.* **9**, 62–82 (Apr. 1990).
2. A. Goswami, B. Espiau and A. Keramane, "Limit Cycles and Their Stability in a Passive Bipedal Gait," *Proceedings of the IEEE International Conference on Robotics and Automation*, IEEE, Minneapolis, MN, USA (1996) pp. 246–251.
3. A. Goswami, B. Espiau and A. Keramane, "Limit cycles in a passive compass gait biped and passivity-mimicking control laws," *Autonom. Rob.* **4**, 273–286 (1997).

https://doi.org/10.1017/S0263574708005079 Published online by Cambridge University Press

4. M. Garcia, A. Chatterjee, A. Ruina and M. J. Coleman, "The simplest walking model: Stability, complexity, and scaling," *ASME J. Biomech. Engg.* **120**, 281–288 (Apr. 1998).
5. A. D. Kuo, "Energetics of actively powered locomotion using the simplest walking model," *ASME J. Biomech. Engg.* **124**, 113–120 (Feb. 2002).
6. M. Wisse, D. G. E. Hobbelen, R. J. J. Rotteveel, S. O. Anderson and G. J. Zeglin, "Ankle Springs Instead of Arc-Shaped Feet for Passive Dynamic Walkers," *Proceedings of IEEE-RAS International Conference on Humanoid Robots*, Genua, Italy (Dec. 2006) pp. 110–116.
7. F. Asano, M. Yamakita, N. Kamamichi and Z.-W. Luo, "A novel gait generation for biped walking robots based on mechanical energy constraint," *IEEE Trans. Rob. Automat.* **20**, 565–573 (2004).
8. F. Asano and Z.-W. Luo, "The Effect of Semicircular Feet on Energy Dissipation by Heel-strike in Dynamic Biped Locomotion," *Proceedings of IEEE International Conference on Robotics and Automation*, Roma, Italy (Apr. 2007) pp. 3976–3981.
9. F. Asano and Z.-W. Luo, "Dynamic analyses of underactuated virtual passive dynamic walking," *Proceedings of IEEE International Conference on Robotics and Automation*, Roma, Italy (Apr. 2007) pp. 3210–3217.
10. M. Wisse, A. L. Schwab and F. C. T. van der Helm, "Passive dynamic walking model with upper body," *Robotica* **22**, 681–688 (2004).
11. S. Takao, H. Ohta, Y. Yokokohji and T. Yoshikawa, "Functional Analysis of Human-Like Mechanical Foot, Using Mechanically Constrained Shoes," *Proceedings of IEEE/RSJ International Conference on Intelligent Robots and Systems*, Sendai, Japan (2004) pp. 3847–3852.
12. J.-W. Yoon, N. Handharu and G. S. Kim, "A Bio-Robotic Toe, Foot and Heel Models of a Biped Robot for more Natural Walking," *Proceedings of the IASTED International Conference on Modeling, Identification and Control 2007*, Innsbruck, Austria (Feb. 2007).
13. K. Nishiwaki, S. Kagami, Y. Kuniyoshi, M. Inaba and H. Inoue, "Toe Joints that Enhance Bipedal and Full-body Motion of Humanoid Robots," *Proceedings of the IEEE International Conference Robotics and Automation*, Washington, DC, USA (May 2002) pp. 3105–3110.
14. R. Sellaouti, O. Stasse, S. Kajita, K. Yokoi and A. Kheddar, "Faster and Smoother Walking of Humanoid HRP-2 with Passive Toe Joints," *Proceedings of the IEEE/RSJ International Conference on Intelligent Robots and Systems*, Beijing, China (Oct. 2006).
15. S. Behnke, "Human-Like Walking using Toes Joint and Straight Stance Leg," *Proceedings of 3rd International Symposium on Adaptive Motion in Animals and Machines*, Ilmenau, Germany (Sep. 2005) pp. 1–6.
16. M. Wisse, C. G. Atkeson and D. K. Kloimwieder, "Swing Leg Retraction Helps Biped Walking Stability," *Proceedings of the IEEE-RAS International Conference on Humanoid Robots*, Tsukuba, Japan (Dec. 2005) pp. 295–300.
17. M. Wisse, A. L. Schwab, R. Q. van der Linde and F. C. T. van der Helm, "How to keep from falling forward: Elementary swing leg action for passive dynamic walkers," *IEEE Trans. Rob.* **21**, 393–401 (2005).
18. M. J. Coleman, A. Chatterjee and A. Ruina, "Motions of a rimless spoked wheel: A simple 3D system with impacts," *Dyn. Stab. Syst.* **12**, 139–160 (1997).
19. A. D. Kuo, "Choosing Your Steps Carefully: Trade-Offs Between Economy and Versatility in Dynamic Walking Bipedal Robots," *IEEE Rob. Automat. Mag.* **14**(2), 18–29 (2007).
20. J. M. Donelan, R. Kram and A. D. Kuo, "Mechanical work for step-to-step transitions is a major determinant of the metabolic cost of human walking," *J. Exp. Biol.* **205**, 3717–3727 (2002).
21. J. E. Pratt and G. A. Pratt, "Exploiting Natural Dynamics in the Control of a 3D Bipedal Walking Simulation," *Proceedings of the International Conference on Climbing and Walking Robots*, Portsmouth, UK (Sep. 1999).

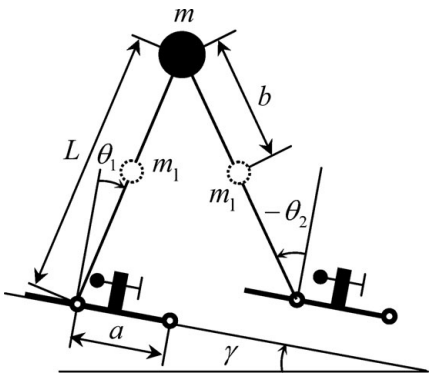


Fig. A1. Model with infinitesimal leg masses and deterministic gait.

Appendix A: Equations of Motion with Nonzero Leg Masses

The equations of motion of the walker during any of the phases can be represented as

$$\boldsymbol{M}(\boldsymbol{\theta})\ddot{\boldsymbol{\theta}} + \boldsymbol{C}(\boldsymbol{\theta}, \dot{\boldsymbol{\theta}})\dot{\boldsymbol{\theta}} + \boldsymbol{g}(\boldsymbol{\theta}; \gamma) = \boldsymbol{\tau} \tag{A1}$$

where $\boldsymbol{\theta} = [\theta_1 \ \theta_2]^T$, θ_2 is the swing leg angle, and θ_1 is the stance leg angle during the ankle joint rotation phase or virtual stance leg angle during toe joint rotation phase. Both θ_1 and θ_2 are measured from vertical as shown in Fig. A1.

The inertia and centrifugal terms are given as follows:

$$\boldsymbol{M}(\boldsymbol{\theta}) = \begin{bmatrix} m_{11} & m_{12} \\ m_{21} & m_{22} \end{bmatrix}, \quad \boldsymbol{C}(\boldsymbol{\theta}, \dot{\boldsymbol{\theta}}) = \begin{bmatrix} c_{11} & c_{12} \\ c_{21} & c_{22} \end{bmatrix}.$$

Let L_h be the length of effective stance leg and α_h be the angle between the effective stance leg and the physical stance leg, which is zero during the ankle joint rotation phase. Let m_1 be the leg mass, which is situated at distance b from the hip joint. Dividing Eq. (A1) with m, and taking the limit $(m_1/m) \to 0$, we get

$$\begin{aligned} m_{11} &= L_\mathrm{h}^2, \quad m_{22} = b^2, \\ m_{12} &= 0, \\ m_{21} &= -bL_\mathrm{h}\cos(\theta_1 - \theta_2), \\ c_{11} &= c_{22} = c_{12} = 0, \\ c_{21} &= bL_\mathrm{h}\dot{\theta}_1 \sin(\theta_1 - \theta_2), \end{aligned}$$

$$\boldsymbol{g}(\boldsymbol{\theta}; \gamma) = \begin{bmatrix} -gL_\mathrm{h}\sin(\theta_1 + \gamma) \\ gb\sin(\theta_2 + \gamma) \end{bmatrix}$$

Appendix B: Transition Equations

The transition equation for impacts is given by

$$\boldsymbol{Q}_\mathrm{p}\dot{\boldsymbol{\theta}}^+ = \boldsymbol{Q}_\mathrm{m}\dot{\boldsymbol{\theta}}^-, \tag{A2}$$

https://doi.org/10.1017/S0263574708005079 Published online by Cambridge University Press

where

$$\boldsymbol{Q}_{\mathrm{m}} = \begin{bmatrix} q_{11}^{-} & q_{12}^{-} \\ q_{21}^{-} & q_{22}^{-} \end{bmatrix}, \quad \boldsymbol{Q}_{\mathrm{p}} = \begin{bmatrix} q_{11}^{+} & q_{12}^{+} \\ q_{21}^{+} & q_{22}^{+} \end{bmatrix}, \tag{A3}$$

and $\dot{\boldsymbol{\theta}}^{-}$, $\dot{\boldsymbol{\theta}}^{+}$ are leg angle vectors before and after the impact. The elements of these matrices for various situations are given as follows.

B.1 Ankle-strike impact

$$q_{11}^{-} = L\cos\alpha_{\mathrm{h}}, \quad q_{12}^{-} = 0,$$
$$q_{21}^{-} = -L\cos(\theta_1^{-} - \theta_2^{-}), \quad q_{22}^{-} = b,$$
$$q_{11}^{+} = L_{\mathrm{v}}, \quad q_{12}^{+} = 0,$$
$$q_{21}^{+} = -L_{\mathrm{v}}\cos(\theta_1^{+} - \theta_2^{+}), \quad q_{22}^{+} = b.$$

B.2 Heel-strike impact

$$q_{11}^{-} = L_{\mathrm{v}}\cos(\theta_1^{-} - \theta_2^{-}), \quad q_{12}^{-} = 0,$$
$$q_{21}^{-} = (b - L_{\mathrm{v}}\cos\alpha_{\mathrm{h}}), \quad q_{22}^{-} = 0,$$
$$q_{11}^{+} = L, \quad q_{12}^{+} = 0,$$
$$q_{21}^{+} = -L\cos(\theta_1^{+} - \theta_2^{+}), \quad q_{22}^{+} = b.$$

https://doi.org/10.1017/S0263574708005079 Published online by Cambridge University Press